Communication in Physical Sciences, 2025, 12(4): 1259-1276

Adsorptive Potential of TiO_2 Nanoparticles for the Removal of Cr (VI) and Pb (II) Metal ions from Fertilizer Wastewater

James Yusuf *, Yisa Jonathan, Jimoh Oladejo Tijani, Razak Bolakale Salau & Elijah Yanda Shaba

Received: 14 March 2025/Accepted: 18 May 2025/Published: 26 May 2025
https://dx.doi.org/10.4314/cps.v12i4.9

Abstract: *Titanium dioxide (TiO_2) nanoparticles have emerged as promising adsorbents for the removal of heavy metal ions from wastewater due to their high surface area, chemical stability and adsorptive properties. The study evaluated the potential of TiO_2 nanoparticles for removing Cr (VI) and Pb (II) from fertilizer wastewater. The TiO_2 nanoparticles was synthesized via green method of synthesis with the highest crystallite size of 15.29 nm under the synthesis condition of a stirring time of 60 min. X-Ray Diffraction (XRD), High-Resolution Transmission Electron Microscopy (HRTEM), Dynamic Light Scattering (DLS), and Energy Dispersive X-Ray Spectroscopy (EDX) were used to characterise the synthesised TiO_2 nanoparticles. HRTEM and XRD analyses of the TiO_2 nanoparticles indicate the formation of spherical shapes and anatase phase crystallite size of 15.29 nm and 12.09 nm for 60 min and 30 min stirring time, respectively. The DLS results show an average particle distribution of 51.54 nm for both stirring time conditions. The EDX revealed the presence of titanium, oxygen and carbon in both stirring times. The synthesized TiO_2 nanoparticles was used as an adsorbent for the removal of Cr (VI) and Pb (II) via batch adsorption. The results indicate that Cr (VI) had a higher adsorption removal efficiency of 52.87 % compared to 40.79 % for Pb (II) at a pH of 6.96, contact time of 30 minutes and a temperature of 30 ^oC. The adsorption isotherm showed that the experimental data fitted best to the Langmuir isotherm as compared to the Freundlich and Dubinin-Radushkevich (D-R) isotherms, demonstrated by higher correlation coefficient values (R^2). The research findings suggest that TiO_2 nanoparticles can be utilized in fertilizer wastewater treatment.*

Keywords*: TiO_2, nanoparticles, anatase, Cr (VI) and Pb (II) removal, fertilizer wastewater and Adsorption Isotherm*

James Yusuf*
Department of Chemistry, Federal University of Technology, PMB 65, Minna, Niger State, Nigeria
Email: **jamesyusuf@kadunapolytechnic.edu.ng**
Orcid id: 009-0009-5531-9602

Yisa Jonathan
Department of Chemistry, Federal University of Technology, PMB 65, Minna, Niger State, Nigeria
Email: yisajo@gmail.com

Jimoh Oladejo Tijani
Nanotechnology Research Group, Africa Centre of Excellence for Mycotoxin and Food Safety, Federal University of Technology, P.M.B 65, Bosso, Minna, Niger State, Nigeria
Email: jimohtijani@futminna.edu.ng

Razak Bolakale Salau
Nanotechnology Research Group, Africa Centre of Excellence for Mycotoxin and Food Safety, Federal University of Technology, P.M.B 65, Bosso, Minna, Niger State, Nigeria
Email: rasaqsalau@futminna.edu.ng

Elijah Yanda Shaba
Department of Chemistry, Federal University of Technology, PMB 65, Minna, Niger State, Nigeria
Email: Elijah.shaba@futminna.edu.ng

1.0 Introduction

The fertilizer industry is a critical component of modern agriculture, providing essential nutrients for crop production through the synthesis of nitrogen, phosphorus, and potassium-based fertilizers. Typically, fertilizer manufacturing involves processes such as ammonia production, nitric acid and phosphoric acid synthesis, and blending with various additives (Kato & Kansha, 2024). However, one of the major environmental challenges associated with this industry is the generation of large volumes of wastewater containing diverse contaminants. It is estimated that approximately 380 billion cubic meters of wastewater are produced annually across all sectors globally, with fertilizer production contributing significantly to this figure (Lim et al., 2021).

Fertilizer wastewater is characterized by high concentrations of nutrients and toxic heavy metals such as chromium (VI), lead (II), cadmium (II), cobalt (II), and zinc (II) (Lim et al., 2021). These heavy metals are primarily introduced into wastewater through raw materials like phosphate rock, industrial chemicals, corrosion of equipment, and process by-products such as fly ash. The presence of heavy metals in wastewater poses serious risks to the environment and human health. When discharged into aquatic systems, these metals can bioaccumulate in the food chain, leading to long-term ecological and health hazards.

Chromium (VI), in particular, is classified as a Group 1 carcinogen by the International Agency for Research on Cancer (IARC). Chronic exposure has been linked to lung cancer, respiratory tract irritation, dermatitis, kidney and liver damage (den Braver-Sewradj et al., 2021; Shekhawat et al., 2015; Shin et al., 2023; Hessel et al., 2021). Similarly, lead (II) and its compounds are highly toxic, causing neurological impairments, developmental disorders in children, enzyme inhibition, and organ damage (Briffa et al., 2020; Mitra et al., 2022). In children, lead exposure has been associated with reduced intelligence quotient (IQ), behavioral issues, and impaired concentration (Ramírez Ortega et al., 2021). Lead also accumulates in bones and soft tissues and enters the human body primarily through contaminated food and water (Collin et al., 2022; Hussaini et al., 2023).

Conventional wastewater treatment methods, including activated carbon adsorption, coagulation-flocculation, activated sludge processes, nanofiltration,photodegradation and reverse osmosis, have been employed to mitigate several contaminants (Gelaw et al., 2024; Eddy *et* al., 2024a-c; Emeka *et* al., 2023; Kolya & Kang, 2023; Kelle *et al*., 2023; Hamdan et al., 2023; Rajkumari et al., 2019; Kumar et al., 2021). However, these methods often face limitations such as high operational costs, sludge generation, membrane fouling, and limited efficiency for complex wastewater matrices containing multiple contaminants (Kesari et al., 2021). As a result, adsorption has gained attention as a more efficient and cost-effective method for heavy metal removal due to its simplicity, ease of operation, and adaptability to various wastewater conditions.

Among the wide range of adsorbents investigated, metal oxide nanoparticles, such as CaO, ZnO, TiO_2 and their composites have shown promising results owing to their high surface area, chemical stability, and non-toxicity (Eddy *et* al., 2023; Naseem & Durrani, 2021; Nuhu *et al*., 2025). TiO_2 nanoparticles are widely applied in water treatment, photocatalysis, solar cells, cosmetics, and pollution remediation (Singh Jassal et al., 2022). The anatase phase of TiO_2, in particular, has demonstrated superior adsorptive and photocatalytic capabilities (Rosa et al., 2024). Recent studies have shown TiO_2's efficacy in removing contaminants such as dyes, organic pollutants, and certain heavy metals, but relatively few studies have focused on its application for removing Cr (VI) and Pb (II) specifically from fertilizer industrial wastewater, despite the severity of these pollutants.

This presents a knowledge gap in the literature concerning the use of green-synthesized TiO_2 nanoparticles for adsorptive removal of these toxic metals under actual industrial wastewater conditions. While studies have reported on synthetic and commercial TiO_2 for water purification, there remains insufficient data on the performance, characterization, and adsorption mechanisms of green-synthesized TiO_2 nanoparticles in complex effluent systems such as those from fertilizer plants.

The aim of this study **is** therefore to evaluate the adsorptive efficiency of green-synthesized TiO_2 nanoparticles for the removal of chromium (VI) and lead (II) ions from fertilizer wastewater. The TiO_2 nanoparticles were synthesized using an environmentally friendly method and characterized using techniques such as X-Ray Diffraction (XRD), High-Resolution Transmission Electron Microscopy (HRTEM), Dynamic Light Scattering (DLS), and Energy Dispersive X-ray Spectroscopy (EDX). The significance of this study lies in its contribution to sustainable wastewater treatment strategies. By utilizing green-synthesized TiO_2 nanoparticles, this work provides insights into low-cost, environmentally benign solutions for heavy metal remediation, which could be adapted by industries to meet environmental regulatory standards and protect public health. Moreover, the findings will expand the scientific understanding of TiO_2-based adsorption systems in the context of fertilizer industry effluents.

2.0 Materials and Methods

2.1 Materials

All chemicals used in this study were of analytical grade and were utilized without further purification. The reagents included titanium tetraisopropoxide (TTIP, $C_{12}H_{28}O_4Ti$, 97%, Central Drug House (P) Ltd.), hydrochloric acid (HCl, 37%, Carlo Erba Reagents, Spain), sodium hydroxide (NaOH, 98.9%, Molychem), ferric chloride ($FeCl_3$, 98.9%, Molychem), and sulfuric acid (H_2SO_4, 98%, Carlo Erba Reagents, Spain).

2.1.1 Sample Collection and Preparation

Fresh stems of *Telfairia occidentalis* (Ugu) were collected from Narayi Market in Chikun Local Government Area, Kaduna State, Nigeria. The plant material was air-dried at ambient temperature (35 ± 2 °C) for three weeks. The dried samples were pulverized using a mortar and pestle to obtain a fine powder. A Soxhlet extraction was performed using 30 g of powdered stem material and 250 mL of ethanol at 50 °C for 6 hours. The ethanolic extract was concentrated using a rotary evaporator and stored in an airtight container for phytochemical analysis and green synthesis of TiO_2 nanoparticles.

2.2 Methods

2.2.1 Phytochemical Screening

Preliminary phytochemical screening of the *Telfairia occidentalis* stem extract was carried out using standard procedures described by Solano et al. (2019), to identify the presence of key phytoconstituents responsible for reduction and stabilization during nanoparticle formation.

2.2.2 Green Synthesis of TiO_2 Nanoparticles

TiO_2 nanoparticles were synthesized via a green method. A 100 mL solution of 1 mol dm^{-3} TTIP was prepared and placed in a 250 mL beaker on a magnetic stirrer. After adjusting the pH with 0.1 mol dm^{-3} NaOH, 20 mL of the *T. occidentalis* stem extract was added dropwise while stirring at 350 rpm for 3 hours. A noticeable color change from pale yellow to deep red-orange indicated nanoparticle formation. The mixture was aged for 24 hours, after which the precipitate was separated by decantation, washed three times with deionized water, and oven-dried at 80 °C for 24 hours. Finally, the dried nanoparticles were calcined at 500 °C for 4 hours in a muffle furnace.

2.2.3 Batch adsorption process

The effects of contact time, nanoadsorbent dosage and temperature on the removal efficiency of Cr (VI) and Pb (II) metal ions from the fertilizer wastewater were examined by a batch adsorption using TiO_2 nanoparticles as an adsorbent. The investigation of contact time on the removal of Cr (VI) and Pb (II), was varied in the range of 15 to 75 min at a constant nanoadsorbent dosage, pH and temperature of 0.06 g, 6.87 and 303 K, respectively. Meanwhile the initial concentration of Cr (VI) and Pb (II) metal ions were 0.159 mg/L and 0.564 mg/L respectively. The effect of the nanoadsorbent dosage on the uptake of Cr (VI) and Pb (II) metal ions from the wastewater was investigated in the range of 0.02 to 0.1 g at the pH (6.87), contact time (30 min) and temperature 30 ^{o}C. In addition, the influence of temperature on the removal of Cr (VI) and Pb (II) metal ions, the temperature was varied in the range of 303 to 343 K under constant conditions of contact time (30 min), nanoadsorbent dose (0.03 g) and pH 6.87. At the end, the samples were digested. Exactly 50 cm^3 of the fertilizer wastewater was measured and transferred into 250 mL beaker and 1:3 of concentrated hydrochloric acid to nitric acid in volume of 5 mL was added. The mixture was heated on a heating mantle at controlled temperature of 80 ^{0}C until the volume reduced to 20 cm^3, then it was allowed to cool and filtered using Whatman filter paper. The solution was made up to the mark of 100 cm^3, and a blank digestion was performed for nitric acid at 80 ^{0}C using the same conditions. The digestion process was carried out in triplicate and Atomic Absorption Spectrophotometer was used to analyse for metal of interest Cr (VI) and Pb (II) metal ions. The removal efficiency (%) and the adsorption capacity (qe mg/g) of Cr (VI) and Pb (II) metal ions in the fertilizer wastewater using the TiO_2 nanoparticles were determined using Eqs. (1) and (2), respectively.

$$\text{Removal Efficiency} = \frac{C_o - C_e}{Co} \times 100 \quad (1)$$

$$q_e = \frac{C_o - C_e}{m} \times v \quad (2)$$

Where C_o (mg/L) and C_e (mg/L) are the initial and equilibrium liquid phase concentration, respectively; V (dm^3) is the volume of the solution and m (g) is the mass of the nanoadsorbents.

2.2.3 Adsorption isotherms

Adsorption isotherms are very helpful for analyzing the adsorption capacities of the adsorbents. When the adsorption equilibrium is established, the relation between the amount of the adsorbates on the adsorbents and the equilibrium concentrations of the adsorbates under constant temperatures is called the adsorption isotherm (Zhu *et al*., 2020). There are various kinds of models for determining the adsorption isotherms, such as the Langmuir, Freundlich, Dubinin–Radushkevich (D-R) and Temkin (Kandasamy *et al*., 2022; Joseph *et al*., 2023; Nannu Shankar *et al*., 2023).

Table 1: Equations for the Isotherm models

Isotherm	**Equation**	
Langmuir	$\frac{C_e}{q_e} = \frac{1}{q_{max} K_L} - \frac{C_e}{q_{max}}$	(3)
Freundlicch	$\mathrm{Iin}(q_e) = \mathrm{Iin}(K_F) + \frac{1}{n}\mathrm{Iin}C_e$	(4)
D-R	$ln q_e = ln q_m - K_{D-R} \varepsilon^2$	(5)

The Langmuir and Freundlich are most extensively used isothern models meanwhile three isotherm models were used in this study nanmely Langmuir, Freundlich and Dubinin–Radushkevich. The Langmuir isotherm model assumes a homogenous monolayer coverage on the surface of the nanoadsorbent without interaction between the adsorbate, while Freundlich isotherm model assumes a multilayer adsorption process on the heterogenous nanoadsorbent surface with different adsorption energies (Boruah *et al*., 2023; Briševac *et al*., 2024). The D-R isotherm determines the mean free energy of adsorption and does not consider the formation of a homogenous layer on the nanoadsorbent surface or that the adsorption is constant (León *et al*., 2023). The equations for the isotherm models of this study are shown in Table 1.

3.0Result and Discussion

3.1 Phytochemical screening of ugu stem plant extracts

The phytochemical screening was carried out to ascertain the bioactive compounds present in the *ugu* stem plant extracts and the result is presented in Table 2.

Table 2: Phytochemical Screening of Ugu stem Plant extract

Phytochemical compounds	Inference	Name of Test
Alkaloids	+	Wagners
Saponins	+	Foam
Phenols	+	Ferric chloride
Flavonoids	+	Alkaline reagent
Tannins	+	Braymer's
Terpenoids	+	Salkowkis

Table 2 shows the presence of bioactive compounds such as alkaloids, flavonoids, saponins, tannins, and terpenoids. These bioactive compounds have the potential to act as capping and stabilizing agents in the synthesis of TiO_2 nanoparticles (Villagrán *et al*., 2024). Different researchers have reported the presence of these bioactive compounds, for instance Bhilkar *et al*. (2023) and Adeyemi *et al*. (2022) reported similar bioactive compounds in the plant extract of *Cymbopogon citratus*

3.2 XRD Analysis of TiO_2 nanoparticles

The mineralogical phases of the TiO_2 nanoparticles synthesized through the green method of synthesis by varying stirring time at 30 minutes and 60 minutes were investigated using XRD and the results are shown in Fig. 1.

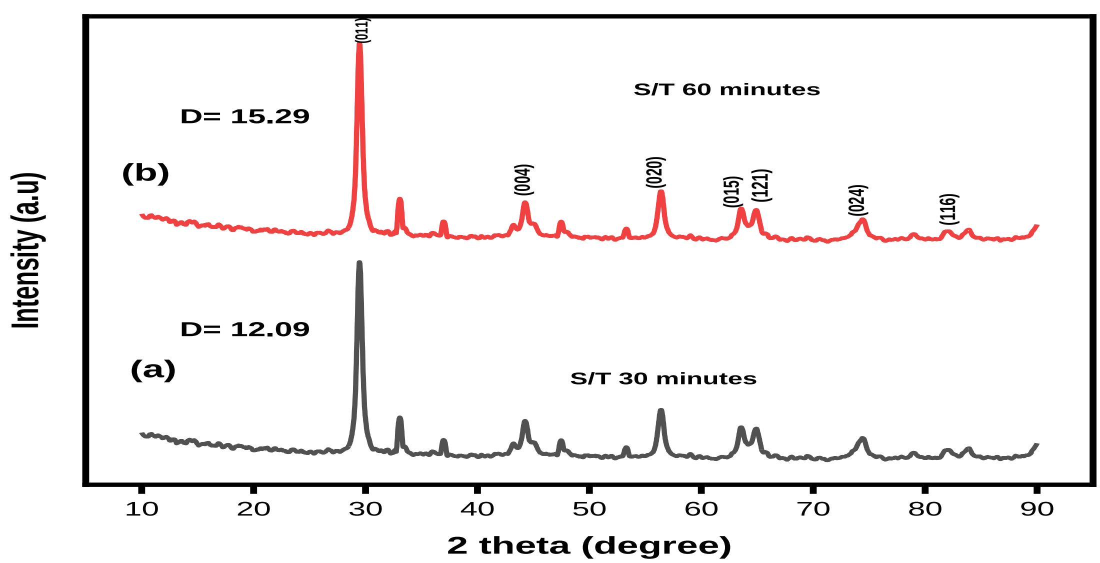

Fig. 1: XRD pattern of TiO_2 Nanoparticles Synthesized at (a) 30 minutes (b) 60 minutes.

The X-ray diffraction pattern of TiO_2 nanoparticles were obtained using *ugu* stem plant extract. Figure 1 shows the presence of peaks at 2 theta value of 29.46°, 43.22°, 56.40°, 63.56° 64.85°, 74.44° and 84.10° corresponding to the miller indices of (011), (004), (020), (015) (121), (024) and (116). These observed peaks agreed with the reference pattern (JCPDS Card No: 00-021-1272) in the XRD literature patterns, which is characteristic of the anatase phase structure of TiO_2 nanoparticles (Nabi *et al*., 2020). The crystallite size of the TiO_2 nanoparticles was calculated to be 12.09 and 15.29 nm using Debye - Scherrer's equation (see equation 6) for the TiO_2 synthesized at 30 and 60 min. The increase in crystallite size as the synthetic time increases may be ascribed to the fact that at longer synthetic times, the TiO_2 nanoparticles have more opportunity to grow through a process known as Ostwald ripening and crystal growth (Shaba *et al*., 2021). As synthesis time increases, the tiny nuclei absorb more atoms or ions from the solution and grow larger.

The mineralogical phase structure obtained is in agreement with the different literature reports on the green synthesis of titanium dioxide nanoparticles using different type of plant extracts *Azadirachta indica*, *Luffa acutangula* and *Acorus calamus* (Tharku *et al*., 2019; Anbumani *et al*., 2022; Ansari *et al*., 2022).

$$D = \frac{0.9\lambda}{\beta Cos\theta} \quad (6)$$

3.3 HRTEM Analysis of TiO_2 Nanoparticles

The internal morphologies of the TiO_2 nanoparticles synthesized were studied by HRTEM and the results are shown in Fig. 2.

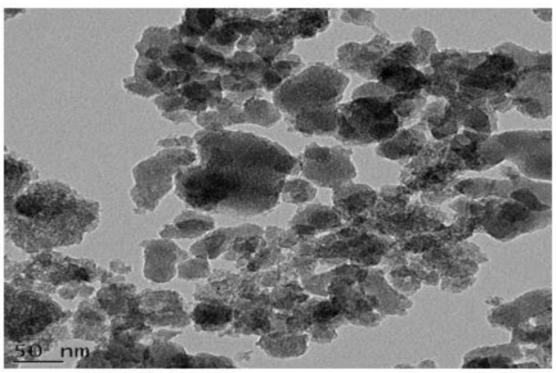

(a)

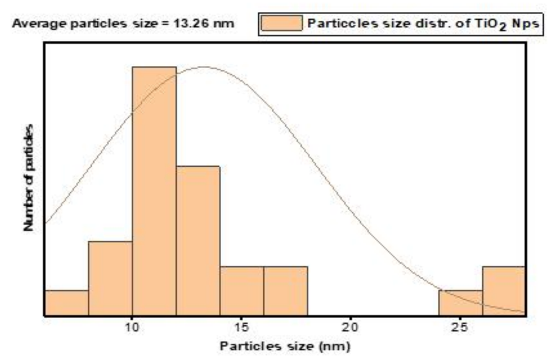

(a1)

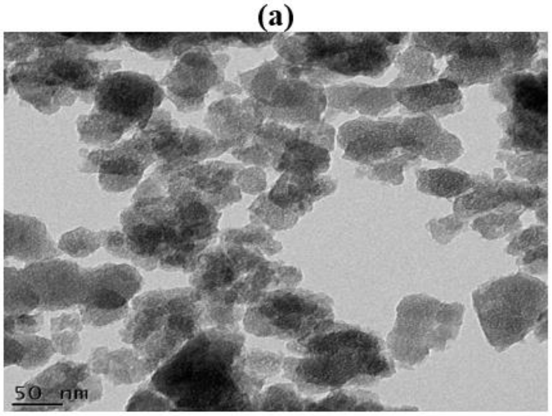

(b)

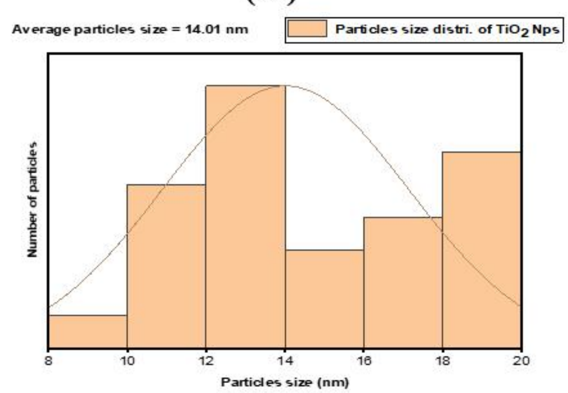

(b1)

Fig. 2: (a) TEM of TiO_2-NPs at 30 minutes (b) TEM of TiO_2-NPs at 60 min

The analysis of internal morphology of the TiO_2 nanoparticles under stirring time of 30 minutes in Figure (a) shows that the synthesized nanoparticles were agglomerated, and their shapes were quasi-nanospheres with particles having a small size but perfectly crystalline in nature and this corresponds to the results reported by several authors in research related to the green synthesis of TiO_2- NPs by the use of aqueous extracts of leaves (Hamdan *et al*., 2020). The TEM results are in close agreement with the average crystallite size obtained from the XRD pattern of the synthesized TiO_2 - NPs.

The images in Figure (b) under stirring 60 minutes also gives clear evidence for the formation of TiO_2-Nps were less agglomerated when compared with the shapes quasi-nanospheres in the above conditions which may be as a result of the increase in the stirring time and this corresponds to the results reported by several authors in research related to the green synthesis of TiO_2 – NPs by the use of aqueous extracts of leaves (Seiß *et al*., 2022; Chen *et al*., 2023).

3.4 EDX Analysis of TiO_2 Nanoparticles

The energy dispersive X–ray was used to analyze the elemental composition of the TiO_2 nanoparticles and the result is shown in Fig. 3.

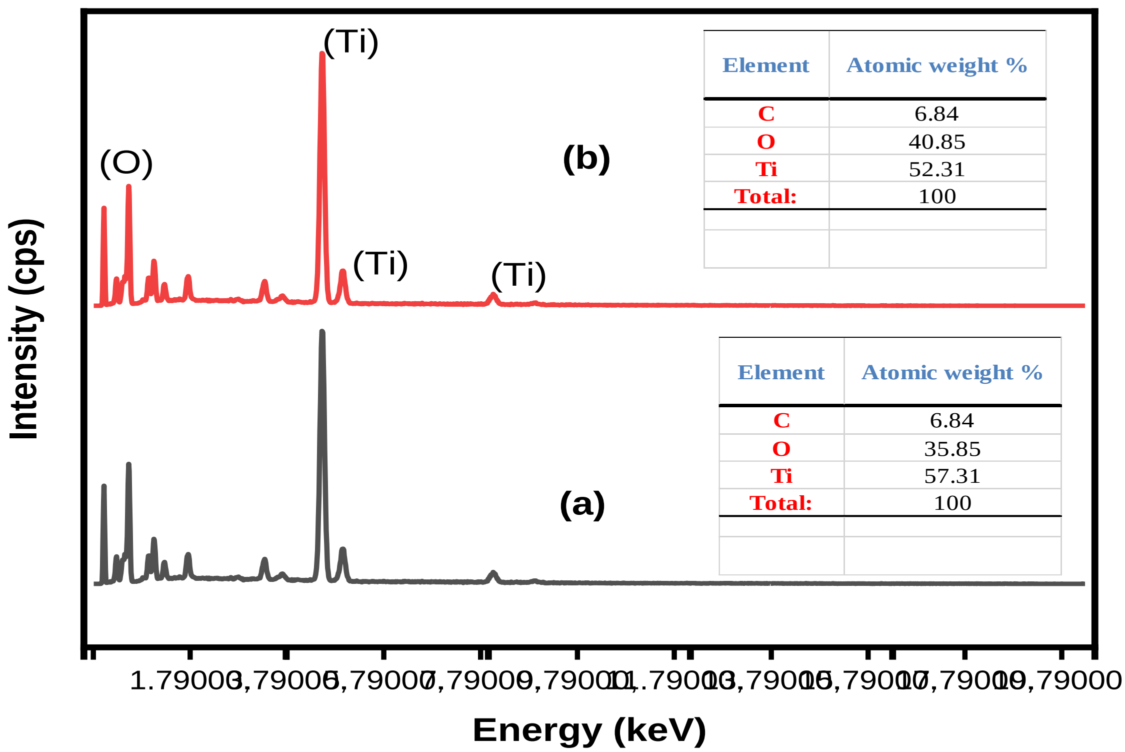

Fig. 3: (a) EDX Analysis of TiO_2-NPs at 60 minutes, (b) 30 minutes

Fig. 3 (a) under stirring time 30 minutes showed that titanium (Ti, 4.01keV) and Oxygen (O, 0.51keV) with percentage composition of Carbon 6.84 %, Oxygen 40.84 % and Titanium 52.31 % correspond to the peaks studied using leaf extract of lemongrass plant (*Cymbopogon citratus)* (Swathi *et al*., 2019). Other element such as carbon might come from the plant extract used in the synthesis process.

Similarly, the separate peaks in Fig. (b) under stirring time 60 minutes showed that titanium appeared at 4.68 keV and oxygen 0.56 keV with percentage composition of carbon 6.84 % , 38.85 % and 57.30 % which is related to the studies carried out using *Ocimum sanctum* leaf extract (Ali *et al*., 2020) and similar investigation was reported by Bahjat (2021) of absorption spectrum of titanium dioxide nanoparticles between 4 KeV and 5KeV using *Sesbania grandiflora* leaf extract. Other element such as carbon which might come from the plant extract used in the synthesis process.

3.5 DLS Analysis of TiO_2 Nanoparticles

The Dynamic Light Scattering was used to analyse for particle size distribution, Poly Dispersity Index (PDI), and hydrodynamic diameter of the TiO_2 nanoparticles and the result is shown in Fig. 4.

The particle size distribution, polydispersity index, and hydrodynamic diameter of synthesized nanoparticles of TiO_2, were analysed using dynamic light scattering. The result shows that the particle size distribution was 51.54 nm as presented in Fig. 4 and the polydispersity index was 0.361 and a significant negative zeta potential of −1.5 mV for both experimental conditions. This negative charge on the developed TiO_2 nanoparticles may be due to the various capping agent from the plant sources present on the surface of nanoparticles.

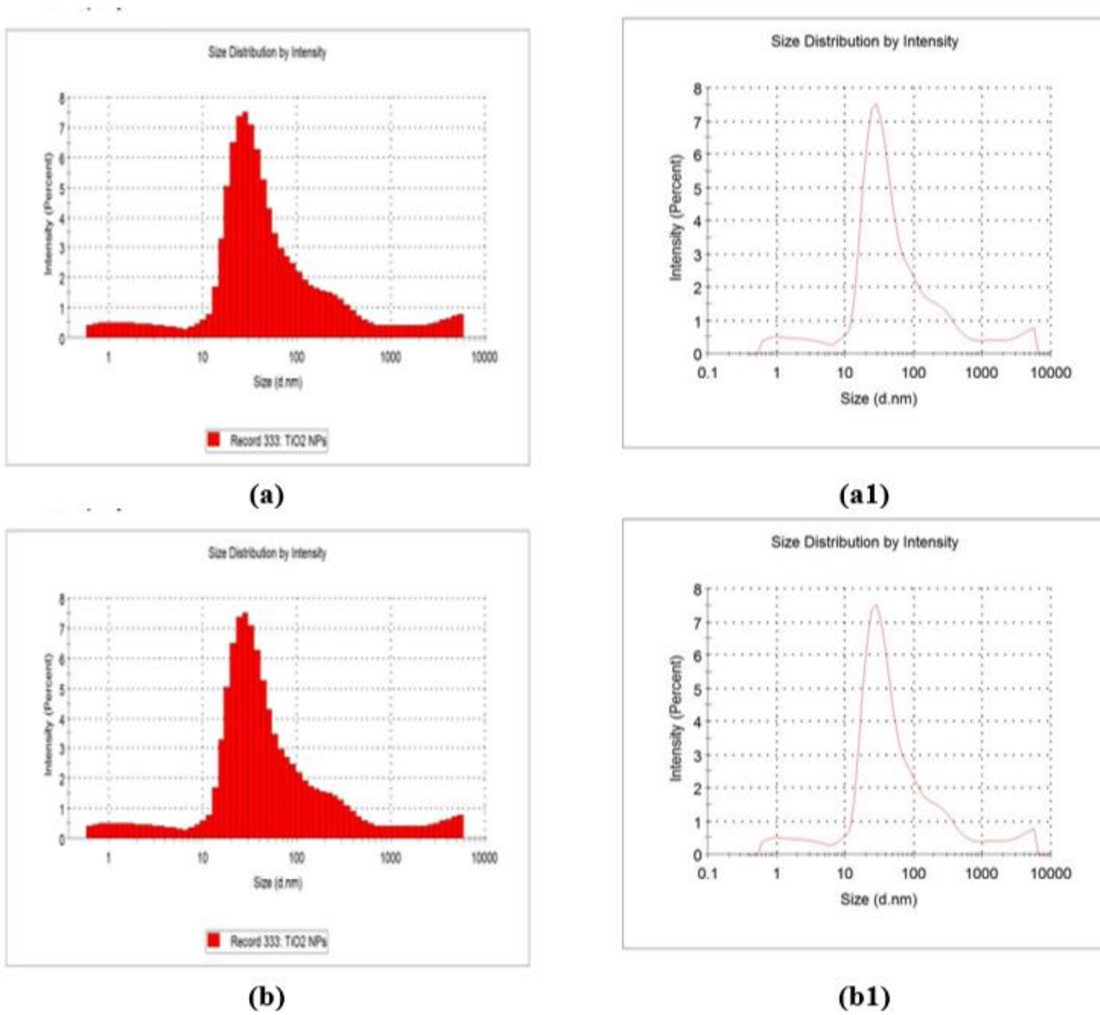

Fig 4: DLS of (a) DLS Analysis of TiO_2-NPs at 30 minutes and (b) 60 minutes

In addition the existence of a significant amount of negative charge on the surface of developed nanoparticles, as demonstrated by the high absolute value of zeta potential, would be helpful in the stability of nanoparticles

(Mohamed *et al.*, 2023; Alengebawy *et al.*, 2021).

3.6 Effect of Contact Time

The influence of contact time on the adsorption efficiencies of Cr (VI) and Pb (II) metal ions from fertilizer wastewater by TiO_2 was studied in the range of 15–75 min under the conditions of nanoadsorbent dosage (0.06 g), pH 6.87 and temperature (303 K) and the result is presented in Figure 5. The removal of Cr (VI) by the nanoadsorbents increased rapidly within the first 15 min and gradually increased until equilibrium was achieved after 45 min of adsorption time while Pb was observed to be rapidly at 15 min and equilibrium was achieved after 30 min of adsorption time. At equilibrium, the highest removal efficiency for Cr (VI) was obtained as 41.23 % and Pb (II) was obtained as 52.65 %. The removal efficiency could be ascribed to significant interaction between the nanoadsorbent and the adsorbate, leading to higher removal of the Cr (VI) and Pb (II) metal ions. As the contact time increased, the metals occupied the active sites leading to it blockage (Egbosiuba *et al.*, 2021). The high percentage removal of Cr (II) mighty be due diffusion and its removal by the nanoadsorbents which could also be explained according to ionic radius of these metals. Element with smaller ionic radius would diffuse faster onto the pores of the nanoadsorbents than element with larger ionic radius (Horsefall *et al.*, 2019). Another possible reason for the differences in the metal ions removed may be due to the nature of the ions in the aqueous medium, ions with smaller sizes have been known to be heavily hydrated and become larger and bulkier than the less hydrated. This less hydration enhanced their chances of being attracted to the adsorption sites faster than the heavily hydrated ions that migrate slowly in aqueous solutions (Bankole *et al.*, 2019). It is also possible that the heavily hydrated ions blocked the small size ions from reaching the binding sites, thus responsible for the low removal efficiency of ions with smaller ionic radii.

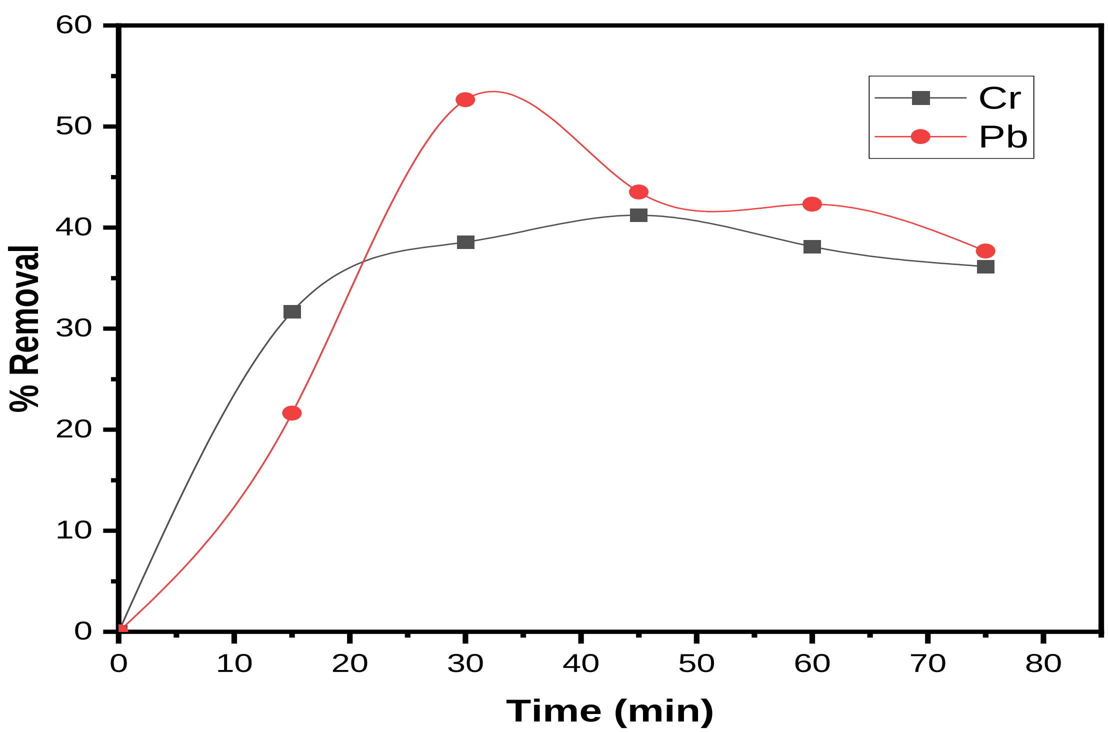

Fig. 5: Variation of %removal with time for the adsorption of Cr (VI) and Pb (II) at pH 6.96 adsorbent dosage (0.06 g) and temperature 30 °C

3.7 Effect of Nanoadsorbent Dosage

Nanoadsorbent dosage is one of the significant factors that affect the efficiency of adsorbents in the removal of pollutants from wastewater (Anoob *et al*., 2024) and was studied in the range of 0.02 – 0.1 g/L at contact time (30 min), pH 6.87 and temperature (30 ^oC). The results are presented in Figure 6 which indicates that the removal efficiencies of Cr (VI) and Pb (II) metal ions using TiO_2 nanoparticles, improved with increasing the dosage from 0.02 to 0.1 g/L. The observed increasing removal trend may be linked to the surface area and the availability of the active site that increase with increasing the nanoadsorbent dosage (Adewoye *et al*., 2021; Zhao *et al*., 2023). The highest percentage adsorption of Cr (VI) was observed to be 73.76 % while Pb was observed to be 45.51 % and were obtained using 0.03 g/L of the TiO_2 nanoparticles. Further increment in the nanoadsorbent dosage up to 0.1 g/L resulted in a decline in the percentage removal which could be attributed to the overlapping of the active sites as reported by Shaba *et al.* (2022) when the nanoadsorbent is increased to an extent, thereby reducing the degree of contact between the nanoadsorbents and the Cr (VI) and Pb (II) metal ions.

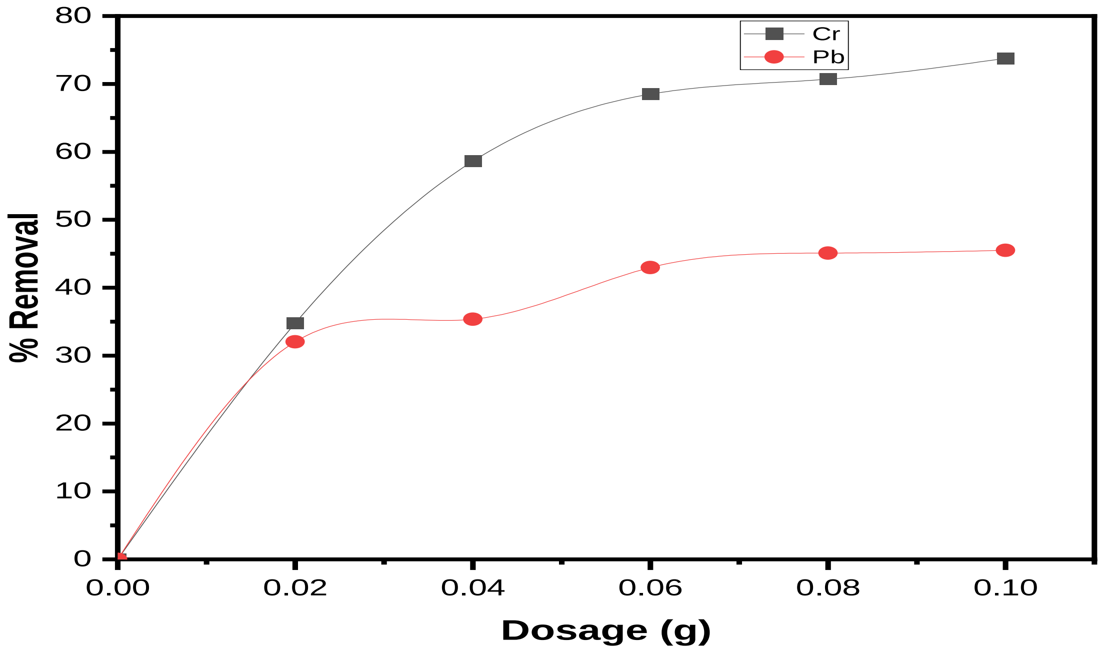

Fig. 6: Variation of %removal with dosage for the adsorption of Cr (VI) and Pb (II) at a constant of pH 6.96 time (30 min) and temperature 30 ^oC.

3.8 Effect of Reaction Temperature

The studies of the adsorption temperature to analyze the endothermic or exothermic nature of the adsorption of Cr (VI) and Pb (II) metal ions from fertilizer wastewater is vital in the adsorption processes (Titus *et al.,* 2021). The effect of different temperatures varied in the range of 30 to 70 ^oC while maintaining previously optimized conditions such as pH (6.87), contact time (30 min), nanoadsorbent dose (0.03 g) and initial metal ions concentration (0.159 mg/L and 0.564 mg/L) on the adsorption of Cr and Pb from fertilizer wastewater was carried out and the results are presented in Figures 7. The findings reveal that increased in percentage removal of Cr (VI) and Pb (II) metal ions increased as the temperature increased from 30 to 70 ^oC. The highest percentage removal of Cr (VI) was observed to be 52.87 % while Pb (II) metal ion was 40.79 %. Therefore, the adsorption of Cr (VI) and Pb (II) metal ions onto the surface of the TiO_2

nanoadsorbents followed an endothermic process (Raji *et al.*, 2023). The observed increase in the adsorption of Cr (VI) and Pb (II) metal ions with increasing temperature may be attributed to the decline in the solution viscosity. This increase the kinetic energy to effectively have contact with the active sites of the nanoadsorbents through diffusion to the interior pores and across the boundary layer (Adebayo *et al.*, 2020; Kandasamy *et al.*, 2022). Many previous studies corroborated the increased adsorption of Cr (VI) and Pb (II) metal ions at elevated temperatures. For instance, Joseph *et al.* (2023) reported the maximum adsorption capacity of Cr (VI) and Pb (II) metal ions at a higher temperature of 350 K.

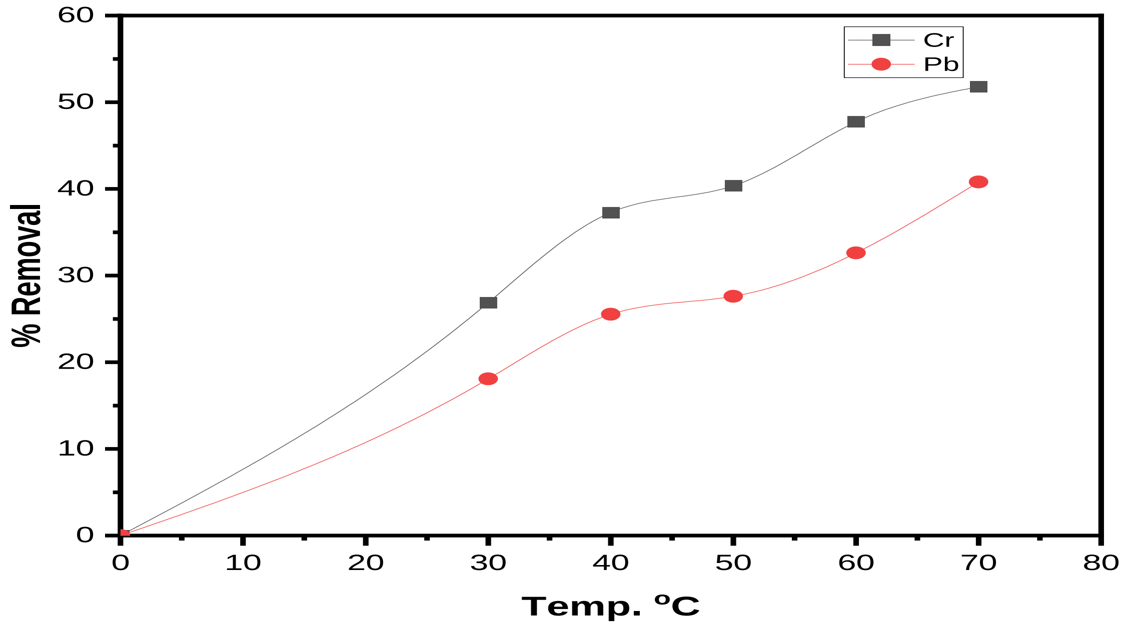

Fig. 5: Variation of % removal with temperature for the adsorption of Cr (VI) and Pb (II) at a constant of pH 6.96 time (30 min) and temperature 30 °C

3.9 Adsorption Isotherm Modelling

Adsorption isotherms were used to demonstrate the relationship between the amount of adsorbate at the point of adsorption equilibrium and the concentration of adsorbate in the aqueous phase. The experimental data were fitted to the Langmuir, Freundlich and Dubinin-Radukevich (D-R) isotherm models to interpret the adsorption behaviour of Cr (VI) and Pb (II) metal ions in the fertilizer wastewater by TiO_2 nanoadsorbent. The results of the isotherm models' equations and estimated adsorption parameters are shown in Table 3. According to the Langmuir isotherm parameters, the Cr (VI) has adsorption capacity (qm) of 0.2694 mg/L while, Pb recorded 0.9280 mg/g. The high adsorption capacity observed in the Pb (II) could attributed to the surface area and the affinity of the Cr and Pb metal ions to the nanoadsorbent. The values 0.2116 dm^3/g and 0.0205 dm^3/g were reported for the KL which indicate a higher affinity of the TiO_2 nanoadsorbent towards Cr (VI) and Pb (II) metal ions. Furthermore, the separation factor (RL) was utilized to confirm the effectiveness of the adsorption process. The value of RL = 0 depicts irreversible adsorption, 0 <RL <1 reflects favorable adsorption and RL >1 refers to an unfavorable adsorption process. Therefore, the values of 0.5993 and 0.1332 were obtained for the removal of Cr (VI) and Pb (II) metal ions respectively which indicate a favorable adsorption process since they are less than one. Freundlich isotherm model assumes a multilayer adsorption process on the heterogeneous nanoadsorbent surface with different adsorption energies (Dada *et al.*, 2021). As seen in Table 3 the value of KF for Cr (VI) was observed to be 1.3510 (mg/g)/(L/mg)1/n while Pb had 2.0193 (mg/g)/(L/mg)1/n. The value of n indicates the adsorption strength of the nanoadsorbent, whereby n < 1 indicates a chemical adsorption process and n >1 indicates a physical adsorption process (Shankar *et al*., 2023). In this study, the Cr (VI) and Pb (II) had chemical adsorption process with values 0.1164 and 0.1103 respectively. In addition higher value of n shows a better adsorption performance by the TiO_2 nanoadsorbent. Similar results have been reported by previous studies (Egbosiuba *et al*., 2021; Wang *et al*., 2024). The D-R isotherm determines the mean free energy of adsorption and does not consider the formation of a homogenous layer on the nanoadsorbent surface or that the adsorption is constant. Here the qs for Cr (VI) metal ions was obtained as 1.0017 mg/g and k_{ad} was obtained as 13.937 mol^2/KJ^2 while qs for Pb (II) metal ions was obtained 1.0108 mg/g and K_{ad} was obtained as 47.793 mol^2/KJ^2. The constant value of ε, affects the chemical or physical determination of an adsorption process and represents the average quantity of energy required for the removal of adsorbed dye molecules from the nanoadsorbent surface. As such, the value of ε <8 kJ/mol indicates physical adsorption, while the value of ε > 8 kJ/mol represents a chemical adsorption process (Raji *et al*., 2023). As shown in Table 3.2, the values of ε obtained for Cr (VI) and Pb (II) metal ions as 1036 and 11625 kJ/mol, respectively indicate the predominant role of chemisorption process in the removal of metal ions by the TiO_2 nanoadsorbent. From the results of this study, it is evident that the experimental data had the best fit with the Langmuir isotherm model due to its high R^2 value. In addition, Langmuir isotherm presented the highest SSE values in comparison with the tested isotherm models, thereby confirming that the adsorption of metal ions was linked to the homogeneous surface of nanoadsorbent with active sites.

Table 3: Kinetics isotherm model for the adsorption of Cr (VI) and Pb (II) from fertilizer wastewater by TiO_2 nanoadsorbent

		TiO_2 nanoadsorbent	
Isotherm Models	Parameters	Cr (VI)	Pb (II)
Langmuir	qm (mg/g)	0.2694	6.9280
	K_L (L/mg)	0.2116	0.0205
	R_L	0.5993	0.1332
	R^2	0.9927	0.9280
	SSE	2.4150	0.0205
Freundlich	KF ((mg/g)/(L/mg)1/n)	1.3510	2.0193
	N	0.1164	0.1103
	R^2	0.8482	0.9421
	SSE	0.1950	0.0109
D –R	qs (mg/g)	1.0017	1.0108
	kad (mol^2/KJ^2)	13.937	47.793
	ε (KJ/mol)	1036	11625
	R^2	0.8144	0.7363
	SSE	0.2385	0.4453

4.0 Conclusion

Titanium dioxide (TiO_2) nanoadsorbent was synthesized via green method of synthesis. X-Ray Diffraction (XRD), High-Resolution Transmission Electron Microscopy (HRTEM), Dynamic Light Scattering (DLS), and Energy Dispersive X-Ray Spectroscopy (EDX) were used to confirm the synthesised TiO_2 nanoadsorbent. The removal of Cr (VI) and Pb (II) via batch adsorption from the fertilizer wastewater was dependent on contact time, adsorbent dosage and temperature. Cr (VI) had a higher adsorption removal efficiency of 52.87 % compared to 40.79 % for Pb (II) at a pH of 6.96, contact time of 30 minutes and a temperature of 30 ^oC. The adsorption data fitted best to the Langmuir isotherm as compared to the Freundlich and Dubinin-Radushkevich (D-R) isotherms, demonstrated by higher correlation coefficient values (R^2). These results shows that TiO_2 nanoadsorbent can be used in fertilizer wastewater treatment.

5.0 References

Abebe, T. G., Tamtam, M. R., Abebe, A. A., Abtemariam, K. A., Shigut, T. G., Dejen, Y. A., & Haile, E. G. (2022). Growing Use and Impacts of Chemical Fertilizers and Assessing Alternative Organic Fertilizer Sources in Ethiopia. *Applied and Environmental Soil Science, 2022.* https://doi.org/10.1155/2022/4738416

Adebayo, G. B., Adegoke, H. I., & Fauzeeyat, S. (2020). Adsorption of Cr(VI) ions onto goethite, activated carbon and their composite: kinetic and thermodynamic studies. *Applied Water Science*, 10, 9, pp. 1–18. https://doi.org/10.1007/s13201-020-01295-z

Adewoye, T. L., Ogunleye, O. O., Abdulkareem, A. S., Salawudeen, T. O., & Tijani, J. O. (2021). Optimization of the adsorption of total organic carbon from produced water using functionalized multi-walled carbon nanotubes. *Heliyon*, 7, 1, , e05866. https://doi.org/10.1016/j.heliyon.2020.e05866

Adeyemi, J. O., Oriola, A. O., Onwudiwe, D. C., & Oyedeji, A. O. (2022). Plant Extracts Mediated Metal-Based Nanoparticles: Synthesis and Biological Applications. *Biomolecules*, *12*, *5*, https://doi.org/10.3390/biom12050627

Alengebawy, A., Abdelkhalek, S. T., Qureshi, S. R., & Wang, M. Q. (2021). **Heavy metals** and pesticides toxicity in agricultural soil and plants: Ecological risks and human health implications. *Toxics*, 9, 3, 42, . https://doi.org/10.3390/toxics9030042.

Ahmed, S. F., Mofijur, M., Ahmed, B., Mehnaz, T., Mehejabin, F., Maliat, D., Hoang, A. T., & Shafiullah, G. M. (2022). Nanomaterials as a sustainable choice for treating wastewater. *Environmental Research*, *214*(July), 113807. https://doi.org/10.1016/j.envres.2022.113807

Al Dawery, S. K., Al-Sawai, M. K., Al Muzami, G. M. S., Annamareddy, S. H. K., Al Dawari, M. S., Harharah, R. H., Harharah, H. N., & Amari, A. (2023). Treatment of Produced Water Using Prepared Activated Carbon-Based Sewage Sludge. *Separations*, 10, 10, https://doi.org/10.3390/separations10100519

Ali, M. A., Ahmed, T., Wu, W., Hossain, A., Hafeez, R., Masum, M. M. I., Wang, Y., An, Q., Sun, G., & Li, B. (2020). Advancements in plant and microbe-based synthesis of metallic nanoparticles and their antimicrobial activity against plant pathogens. *Nanomaterials*, 10, 6, pp. 1–24. https://doi.org/10.3390/nano10061146

Anoob, F., Arachchi, S., Azamathulla, H. M., Al-mahbashi, N., & Rathnayake, U. (2024). Nanoadsorbents as an effective wastewater treatment candidate for pharmaceutical contaminants; towards sustainable policy development. *Case Studies in Chemical and Environmental Engineering*, *9*(December 2023), 100639.

https://doi.org/10.1016/j.cscee.2024.100639

Bahjat, H. H. (2021). *Magnetic Field – Assisted Laser Ablation of Titanium Dioxide Nanoparticles in Water for Anti- Bacterial Applications*.

Bankole, M. T., Abdulkareem, A. S., Mohammed, I. A., Ochigbo, S. S., Tijani, J. O., Abubakre, O. K., & Roos, W. D. (2019). Selected Heavy Metals Removal From Electroplating Wastewater by Purified and Polyhydroxylbutyrate Functionalized Carbon Nanotubes Adsorbents. *Scientific Reports*, 9, 1, pp. 1–19. https://doi.org/10.1038/s41598-018-37899-4

Bhilkar, P. R., Bodhne, A. S., Yerpude, S. T., Madankar, R. S., Somkuwar, S. R., Daddemal-Chaudhary, A. R., Lambat, A. P., Desimone, M., Sharma, R., & Chaudhary, R. G. (2023). Phyto-derived metal nanoparticles: Prominent tool for biomedical applications. *OpenNano*, *14*(June), 100192. https://doi.org/10.1016/j.onano.2023.100192

Bogusz, P., Rusek, P., & Brodowska, M. S. (2021). Suspension fertilizers: How to reconcile sustainable fertilization and environmental protection. *Agriculture (Switzerland)*, 11, 10, pp. 1–14. https://doi.org/10.3390/agriculture11101008

Boruah, H., Tyagi, N., Gupta, S. K., Chabukdhara, M., & Malik, T. (2023). Understanding the adsorption of iron oxide nanomaterials in magnetite and bimetallic form for the removal of arsenic from water. *Frontiers in Environmental Science*, 11, pp. 1–21. https://doi.org/10.3389/fenvs.2023.1104320

Briffa, J., Sinagra, E., & Blundell, R. (2020). Heavy metal pollution in the environment and their toxicological effects on humans. *Heliyon*, *6*, *9*, e04691. https://doi.org/10.1016/j.heliyon.2020.e04691

Briševac, D., Gabelica, I., Ljubas, D., Bafti, A., Matijašić, G., & Ćurković, L. (2024). Effects of TiO2 Nanoparticles Synthesized via Microwave Assistance on Adsorption and Photocatalytic Degradation of Ciprofloxacin. *Molecules (Basel, Switzerland)*, 29, 12, . https://doi.org/10.3390/molecules29122935

Chen, B., Li, L., Liu, L., & Cao, J. (2023). Effective adsorption of heavy metal ions in water by sulfhydryl modified nano titanium dioxide. *Frontiers in Chemistry*, 10, pp. 1–10. https://doi.org/10.3389/fchem.2022.1072139

Collin, S., Baskar, A., Geevarghese, D. M., Ali, M. N. V. S., Bahubali, P., Choudhary, R., Lvov, V., Tovar, G. I., Senatov, F., Koppala, S., & Swamiappan, S. (2022). Bioaccumulation of lead (Pb) and its effects in plants: A review. *Journal of Hazardous Materials Letters*, 3, 100064. https://doi.org/10.1016/j.hazl.2022.100064

Dada, A. O., Adekola, F. A., Odebunmi, E. O., Ogunlaja, A. S., & Bello, O. S. (2021). Two–three parameters isotherm modeling, kinetics with statistical validity, desorption and thermodynamic studies of adsorption of Cu(II) ions onto zerovalent iron nanoparticles. *Scientific Reports*, 11, pp. 1–15. https://doi.org/10.1038/s41598-021-95090-8

den Braver-Sewradj, S. P., van Benthem, J., Staal, Y. C. M., Ezendam, J., Piersma, A. H., & Hessel, E. V. S. (2021). Occupational exposure to hexavalent chromium. Part II. Hazard assessment of carcinogenic effects. *Regulatory Toxicology and Pharmacology*, 126, 105045. https://doi.org/10.1016/j.yrtph.2021.105045

Eddy, N. O., Garg, R., Ukpe, R. A., Ameh, P. O., Gar, R., Musa, R., Kwanchi, D., Wabaidur, S. M., Afta, S., Ogbodo, R., Aikoye, A. O., & Siddiqu, M. (2024a).

Application of periwinkle shell for the synthesis of calcium oxide nanoparticles and in the remediation of Pb2+-contaminated water. *Biomass Conversion and Biorefinery*. https://doi.org/10.1007/s13399-024-05285-y

Eddy, N. O., Jibrin, J. I., Ukpe, R. A., Odiongenyi, A., Iqbal, A., Kasiemobi, A. M., Oladele, J. O., & Runde, M. (2024b). Experimental and Theoretical Investigations of Photolytic and Photocatalysed Degradations of Crystal Violet Dye (CVD) in Water by oyster shells derived CaO nanoparticles (CaO-NP). *Journal of Hazardous Materials Advances*, 13, 100413. https://doi.org/10.1016/j.hazadv.2024.100413

Eddy, N. O., Oladede, J., Eze, I. S., Garg, R., Garg, R., & Paktin, H. (2024c). Synthesis and characterization of CaO nanoparticles from periwinkle shell for the treatment of tetracycline-contaminated water by adsorption and photocatalyzed degradation. *Results in Engineering*, 103374. https://doi.org/10.1016/j.rineng.2024.103374

Eddy, N. O., Ukpe, R. A., Ameh, P., Ogbodo, R., Garg, R., & Garg, R. (2023). Theoretical and experimental studies on photocatalytic removal of methylene blue (MetB) from aqueous solution using oyster shell synthesized CaO nanoparticles (CaONP-O). *Environmental Science and Pollution Research*. https://doi.org/10.1007/s11356-022-22747-w

Egbosiuba, T. C., Abdulkareem, A. S., Kovo, A. S., Afolabi, E. A., Tijani, J. O., Bankole, M. T., Bo, S., & Roos, W. D. (2021). Adsorption of Cr(VI), Ni(II), Fe(II) and Cd(II) ions by KIAgNPs decorated MWCNTs in a batch and fixed bed process. *Scientific Reports*, 11, 1, pp. 1–20. https://doi.org/10.1038/s41598-020-79857-z

Gelaw, Y. B., Dagne, H., Adane, B., Yirdaw, G., Moges, M., Aneley, Z., Kumlachew, L., Aschale, A., Deml, Y. A., Tegegne, E., & Birhan, T. A. (2024). Adsorptive removal of cadmium (II) from wastewater using activated carbon synthesized from stem of Khat (Catha edulis). *Heliyon*, 10, 22, e40389. https://doi.org/10.1016/j.heliyon.2024.e40389

Hamdan, M. A., Sublaban, E. T., Al-Asfar, J. J., & Banisaid, M. A. (2023). Wastewater Treatment Using Activated Carbon Produced from Oil Shale. *Journal of Ecological Engineering*, 24, 2, pp. 131–139. https://doi.org/10.12911/22998993/156664

Hamdan, S. A., Ibrahim, I. M., & Ali, I. M. (2020). Comparison of anatase and rutile TiO2 nanostructure for gas sensing application. *Digest Journal of Nanomaterials and Biostructures*, 15, 4, pp. 1001–1008. https://doi.org/10.15251/djnb.2020.154.1001

Hessel, E. V. S., Staal, Y. C. M., Piersma, A. H., den Braver-Sewradj, S. P., & Ezendam, J. (2021). Occupational exposure to hexavalent chromium. Part I. Hazard assessment of non-cancer health effects. *Regulatory Toxicology and Pharmacology*, 126, 105048. https://doi.org/10.1016/j.yrtph.2021.105048

Hussaini, A. B., Cao, J., Yateh, M., & Wu, B. (2023). Effects of Industrial Wastewater Effluents on Irrigation Water Quality around Bompai Industrial Area, Kano State, Nigeria. *OALib*, 10, 07, pp. 1–14. https://doi.org/10.4236/oalib.1110395

Joseph, T. N., Isaiah, O. B., & Sammy, L. C. (2023). Chromium (VI) adsorption from steel industry wastewater using biomass and agro-based adsorbents: A Review. *Journal of Agriculture, Science and Technology*, 23, 1, pp. 50–76. https://doi.org/10.4314/jagst.v23i1.5

Kandasamy, S., Velusamy, S., Thirumoorthy, P., Periyasamy, M., Senthilkumarveerasamy, Gopalakrishnan, K. M., Sathish, U., Kiramani, V., Antrini, F. D. G., & Periyasamy, S. (2022). Adsorption of Chromium Ions from Aqueous Solutions by Synthesized Nanoparticles. *Journal of Nanomaterials, 2022*. https://doi.org/10.1155/2022/6214 -438

Kato, S., & Kansha, Y. (2024). Comprehensive review of industrial wastewater treatment techniques. *Environmental Science and Pollution Research*, 31, 37, pp. 51064–51097. https://doi.org/10.1007/s11356-024-34584-0

Kelle, H. I., Ogoko, E. C., Akintola O, & Eddy, N. O. (2023). Quantum and experimental studies on the adsorption efficiency of oyster shell–based CaO nanoparticles (CaONPO) towards the removal of methylene blue dye (MBD) from aqueous solution. *Biomass Conversion and Biorefinery*. https://doi.org/10.1007/s13399-023-04947-7

Kesari, K. K., Soni, R., Jamal, Q. M. S., Tripathi, P., Lal, J. A., Jha, N. K., Siddiqui, M. H., Kumar, P., Tripathi, V., & Ruokolainen, J. (2021). Sci-Hub | Wastewater Treatment and Reuse: a Review of its Applications and Health Implications. *Water, Air, & Soil Pollution, 232, 5,* 208. https://doi.org/10.1007/s11270-021-05154-8

Kolya, H., & Kang, C. W. (2023). Bio-Based Polymeric Flocculants and Adsorbents for Wastewater Treatment. *Sustainability (Switzerland)*, 15, *12*, https://doi.org/10.3390/su15129844

Kumar Dadarwal Sri Karan, B., Bahuguna, A., Singh, S., Bahuguna, A., Sharma, S., & Kumar Dadarwal, B. (2021). Physical method of Wastewater treatment-A review. *Quest Journals Journal of Research in Environmental and Earth Sciences*, 7, 6, pp. 2348–2532.

León, A. Y., Contreras-Arenas, J. D., Garnica-Fuentes, C. F., Jiménez-Caballero, M. A., Pinto-Hernández, D. F., Ariza-León, E., Peña-Ballesteros, D. Y., & Molina-Velasco, D. R. (2023). Removal of organic compounds in wastewater using cocoa shell-based activated carbon–SiO2 nanoparticles. *Environment, Development and Sustainability*, 0123456789. https://doi.org/10.1007/s10668-023-04168-y

Lim, J., Fernandez, C., & Hatzell, M. (2021). Ammonia and Nitric Acid Demands for Fertilizer Use in 2050. *ACS Energy Letters*, *6*, pp.3676–3685. https://doi.org/10.1021/acsenergylett.1c01614

Mitra, S., Chakraborty, A. J., Tareq, A. M., Emran, T. Bin, Nainu, F., Khusro, A., Idris, A. M., Khandaker, M. U., Osman, H., Alhumaydhi, F. A., & Simal-Gandara, J. (2022). Impact of heavy metals on the environment and human health: Novel therapeutic insights to counter the toxicity. *Journal of King Saud University - Science*, 34, 3, 101865. https://doi.org/10.1016/j.jksus.2022.101865

Mohamed, A., Atta, R. R., Kotp, A. A., Abo El-Ela, F. I., Abd El-Raheem, H., Farghali, A., Alkhalifah, D. H. M., Hozzein, W. N., & Mahmoud, R. (2023). Green synthesis and characterization of iron oxide nanoparticles for the removal of heavy metals (Cd2+ and Ni2+) from aqueous solutions with Antimicrobial Investigation. *Scientific Reports*, 13, 1, pp. 1–30. https://doi.org/10.1038/s41598-023-31704-7

Nabi, G., Raza, W., & Tahir, M. B. (2020). Green Synthesis of TiO2 Nanoparticle Using Cinnamon Powder Extract and the Study of Optical Properties. *Journal of Inorganic and Organometallic Polymers and Materials*, 30, 4, pp. 1425–1429. https://doi.org/10.1007/s10904-019-01248-3

Nannu Shankar, S., Dinakaran, D. R., Chandran, D. K., Mantha, G., Srinivasan, B., & Nyayiru Kannaian, U. P. (2023). Adsorption kinetics, equilibrium and thermodynamics of a textile dye V5BN by a natural nanocomplex material: Clinoptilolite. *Energy Nexus*, 10, , 100197. https://doi.org/10.1016/j.nexus.2023.100197

Naseem, T., & Durrani, T. (2021). The role of some important metal oxide nanoparticles for wastewater and antibacterial applications: A review. *Environmental Chemistry and Ecotoxicology*, *3*, pp.59–75. https://doi.org/10.1016/j.enceco.2020.12.001

Nuhu, J. S., Awe, F. E., Garg, R., Garg, R., Eddy, N. O., & Paktin, H. (2025). Cobalt titanate nanocatalyst for enhanced photodegradation of atrazine: Kinetics, degradation efficiency, and mechanistic analysis. *BMC Chemistry*, *19*, 31. https://doi.org/10.1186/s13065-025-01394-5

Ogoko, E. C., Kelle, H. I., Akintola, O., & Eddy, N. O. (2023). Experimental and theoretical investigation of *Crassostrea gigas* (gigas) shells based CaO nanoparticles as a photocatalyst for the degradation of bromocresol green dye (BCGD) in an aqueous solution. *Biomass Conversion and Biorefinery*. https://doi.org/10.1007/s13399-023-03742-8

Raji, Z., Karim, A., Karam, A., & Khalloufi, S. (2023). Adsorption of Heavy Metals: Mechanisms, Kinetics, and Applications of Various Adsorbents in Wastewater Remediation—A Review. *Waste*, *1*, 3, pp. 775–805. https://doi.org/10.3390/waste1030046

Rajkumari, J., Magdalane, C. M., Siddhardha, B., Madhavan, J., Ramalingam, G., Al-Dhabi, N. A., Arasu, M. V., Ghilan, A. K. M., Duraipandiayan, V., & Kaviyarasu, K. (2019). Synthesis of titanium oxide nanoparticles using Aloe barbadensis mill and evaluation of its antibiofilm potential against Pseudomonas aeruginosa PAO1. *Journal of Photochemistry and Photobiology B: Biology*, 201, 111667. https://doi.org/10.1016/j.jphotobiol.2019.111667

Ramírez Ortega, D., González Esquivel, D. F., Blanco Ayala, T., Pineda, B., Gómez Manzo, S., Marcial Quino, J., Carrillo Mora, P., & Pérez de la Cruz, V. (2021). Cognitive impairment induced by lead exposure during lifespan: Mechanisms of lead neurotoxicity. *Toxics*, 9, 2, pp. 1–30. https://doi.org/10.3390/toxics9020023

Rosa, D., Abbasova, N., & Di Palma, L. (2024). Titanium Dioxide Nanoparticles Doped with Iron for Water Treatment via Photocatalysis: A Review. *Nanomaterials*, 14, 3, https://doi.org/10.3390/nano14030293

Seiß, V., Thiel, S., & Eichelbaum, M. (2022). Preparation and Real World Applications of Titania Composite Materials for Photocatalytic Surface, Air, and Water Purification: State of the Art. *Inorganics*, 10, 9, https://doi.org/10.3390/inorganics10090139

Shaba, E. Y., Tijani, J. O., Jacob, J. O., & Suleiman, M. A. T. (2022). Simultaneous removal of Cu (II) and Cr (VI) ions from petroleum refinery wastewater using ZnO/Fe3O4 nanocomposite. *Journal of Environmental Science and Health - Part A Toxic/Hazardous Substances and Environmental Engineering*, 57, 13, 14, pp. 1146–1167. https://doi.org/10.1080/10934529.2022.2162794

Shekhawat, K., Chatterjee, S., & Joshi, B. (2015). Chromium Toxicity and its Health Hazards Manuscript Info Abstract. *June*.

Shin, D. Y., Lee, S. M., Jang, Y., Lee, J., Lee, C. M., Cho, E. M., & Seo, Y. R. (2023). Adverse Human Health Effects of Chromium by Exposure Route: A

Comprehensive Review Based on Toxicogenomic Approach. *International Journal of Molecular Sciences*, 24, 4, https://doi.org/10.3390/ijms24043410

Singh Jassal, P., Kaur, D., Prasad, R., & Singh, J. (2022). Green synthesis of titanium dioxide nanoparticles: Development and applications. *Journal of Agriculture and Food Research*, 10, 100361. https://doi.org/10.1016/j.jafr.2022.100361

Solano, R. A., Herrera, A. P., Maestre, D., & Cremades, A. (2019). Fe-TiO 2 Nanoparticles Synthesized by Green Chemistry for Potential Application in Waste Water Photocatalytic Treatment. *Journal of Nanotechnology*, *2019*. https://doi.org/10.1155/2019/4571848

Swathi, N., Sandhiya, D., Rajeshkumar, S., & Lakshmi, T. (2019). Green synthesis of titanium dioxide nanoparticles using Cassia fistula and its antibacterial activity. *International Journal of Research in Pharmaceutical Sciences*, 10, 2, pp. 856–860. https://doi.org/10.26452/ijrps.v10i2.261

Villagrán, Z., Miguel Anaya-Esparza, L., Arnulfo Velázquez-Carriles, C., Manuel Silva-Jara, J., Martín Ruvalcaba-Gómez, J., Aurora-Vigo, E. F., Rodríguez-Lafitte, E., Rodríguez-Barajas, N., & Balderas-León, I. (2024). Use of Plant-Based Extracts as Reducing, Capping, and Stabiliz-2 ing Agents for the Green Synthesis of Inorganic Nanoparticles 3. *13*.

Wang, C., Chen, J., & Yang, Q. (2024). Iron-Based MOF : Ion Branching and Domain-Limiting Effects. *Vi*.

Zhao, W., Hao, C., Guo, Y., Shao, W., Tian, Y., & Zhao, P. (2023). Optimization of Adsorption Conditions Using Response Surface Methodology for Tetracycline Removal by MnFe2O4/Multi-Wall Carbon Nanotubes. *Water (Switzerland)*, *15*, 13. https://doi.org/10.3390/w15132392

Zhu, Y., Yang, Q., Lu, T., Qi, W., Zhang, H., Wang, M., Qi, Z., & Chen, W. (2020). Effect of phosphate on the adsorption of antibiotics onto iron oxide minerals: Comparison between tetracycline and ciprofloxacin. *Ecotoxicology and Environmental Safety*, *205*, 111345. https://doi.org/10.1016/j.ecoenv.2020.111345

Compliance with Ethical Standards Declaration

Ethical Approval

Not Applicable

Competing interests

The authors declare no known competing financial interests

Data Availability

Data shall be made available on request

Conflict of Interest

The authors declare no conflict of interest

Ethical Considerations

Not applicable

Funding

The authors declared no external source of funding.

Authors' Contributions

James Yusuf: Conceived, designed the experiments, performed the experiments and wrote the paper; Analyzed and interpreted the data.

Yisa Jonathan and Jimoh Oladejo Tijani: Analyzed and interpreted the data. Razak Bolakale Salau and Elijah Yanda Shaba: Analyzed and interpreted the data.